available at www.sciencedirect.com

SCIENCE DIRECT®

journal homepage: www.elsevier.com/locate/biochempharm

Distribution of tocopheryl quinone in mitochondrial membranes and interference with ubiquinone-mediated electron transfer

Wolfgang Gregor, Katrin Staniek, Hans Nohl, Lars Gille *

Research Institute for Biochemical Pharmacology and Molecular Toxicology, University of Veterinary Medicine Vienna, Austria

ARTICLE INFO

Article history:
Received 22 December 2005
Accepted 20 February 2006

Keywords:
Mitochondria
α-Tocopherol
α-Tocopheryl quinone
Ubiquinone
Respiratory complexes

Abbreviations:
BHT, 3,5-di-*tert*-butyl-4-hydroxy-toluol
Cox, cytochrome *c* oxidase
Cyt, cytochrome
DETAPAC, diethylene-triamino-pentaacetic acid
FAD, flavin adenine dinucleotide
FMN, flavin mononucleotide
HPLC, high performance liquid chromatography
IM, mitochondrial inner membrane
$k_{cat,app}$, apparent turnover number
$K_{M,app}$, apparent (bulk phase) Michaelis constant
MAO, monoamine oxidase
MP, mitoplasts
OM, mitochondrial outer membrane
RHM, rat heart mitochondria
RLM, rat liver mitochondria

ABSTRACT

α-Tocopherol (Toc) is an efficient lipophilic antioxidant present in all mammalian lipid membranes. This chromanol is metabolized by two different pathways: excessive dietary Toc is degraded in the liver by side chain oxidation, and Toc acting as antioxidant is partially degraded to α-tocopheryl quinone (TQ). The latter process and the similarity between TQ and ubiquinone (UQ) prompted us to study the distribution of TQ in rat liver mitochondrial membranes and the interference of TQ with the activity of mitochondrial and microsomal redox enzymes interacting with UQ. In view of the contradictory literature results regarding Toc, we determined the distribution of Toc, TQ, and UQ over inner and outer membranes of rat liver mitochondria. Irrespective of the preparation method, the TQ/Toc ratio tends to be higher in mitochondrial inner membranes than in outer membranes suggesting TQ formation by respiratory oxidative stress in vivo. The comparison of the catalytic activities using short-chain homologues of TQ and UQ showed decreasing selectivity in the order complex II (TQ activity not detected) > Q_o site of complex III > Q_i site of complex III > complex I ~ cytochrome b_5 reductase > cytochrome P-450 reductase (comparable reactivity of UQ and TQ). TQ binding to some enzymes is comparable to UQ despite low activities. These data show that TQ arising from excessive oxidative degradation of Toc can potentially interfere with mitochondrial electron transfer. On the other hand, both microsomal and mitochondrial enzymes contribute to the reduction of TQ to tocopheryl hydroquinone, which has been suggested to play an antioxidative role itself.

* *Corresponding author at*: Research Institute for Biochemical Pharmacology and Molecular Toxicology, University of Veterinary Medicine Vienna, Veterinärplatz 1, A-1210 Vienna, Austria. Tel.: +43 1 25077 4407; fax: +43 1 25077 4490.
E-mail address: Lars.Gille@vu-wien.ac.at (L. Gille).

0006-2952/$ – see front matter © 2006 Elsevier Inc. All rights reserved.
doi:10.1016/j.bcp.2006.02.012

S.D., standard deviation
SMP, submitochondrial particles
Toc, α-tocopherol
TQ, α-tocopheryl quinone
UQ, ubiquinone
V_{max}, maximal velocity

1. Introduction

Mitochondria are generally considered as origin but also as target for reactive oxygen species [1,2]. Ubisemiquinones and iron sulfur centers of the mitochondrial respiratory chain have been suggested to trigger the formation of superoxide radicals under certain (patho-)physiological conditions [3–5]. On the other hand it has been demonstrated that the mitochondrial production of ATP is very sensitive to protein thiol oxidation, which deteriorates enzyme functions, and to lipid peroxidation, which uncouples electron transfer from ATP production by unspecific proton back-flow [6–8]. Therefore, mitochondrial antioxidants are particularly responsible for the maintenance of these essential functions. Thiol groups, often exposed to an aqueous environment, are protected by antioxidant enzymes and glutathione (GSH). The integrity of the lipid membrane is preserved by the combined action of α-tocopherol (Toc) and ubiquinol (UQH_2) as antioxidants. Rate constants with peroxyl radicals are $3.3 \times 10^6\ M^{-1}\ s^{-1}$ for Toc and $3.4 \times 10^5\ M^{-1}\ s^{-1}$ for UQ_9H_2 [9], suggesting that the preferential radical scavenger in mitochondrial membranes is Toc [10]. In contrast, other reports describe that the reactivities of Toc and UQH_2 towards the model radical galvinoxyl strongly depend on the environment. In ethanol, which simulates the polar components of membranes, the rate constants are comparable ($5.12 \times 10^3\ M^{-1}\ s^{-1}$ for Toc; $5.19 \times 10^3\ M^{-1}\ s^{-1}$ for $UQ_{10}H_2$), but in hexane, which mimics the apolar membrane core, Toc is about 10 times more efficient than UQH_2 ($1.94 \times 10^5\ M^{-1}\ s^{-1}$ for Toc; $2.11 \times 10^4\ M^{-1}\ s^{-1}$ for $UQ_{10}H_2$) [11]. Furthermore, the chromanoxyl radical of Toc (tocopheroxyl) is efficiently recycled by ubiquinol, and ubiquinol is regenerated by the respiratory chain. Therefore, this mitochondrial redox carrier is important for the antioxidant defense [12,13].

In spite of this efficient recycling system it was repeatedly shown that the two-electron oxidation product of Toc, α-tocopheryl quinone (TQ; sometimes referred to as tocopherol quinone or Vitamin E quinone; see Scheme 1), which presumably cannot be recycled back to Toc (but see Refs. [14,15]), exists in mitochondrial membranes [16–18], but also in the endoplasmic reticulum [18,19], in plasma [20] and in microorganisms [21]. Several reports have shown that TQ could arise both from the diet [22] and from intracellular oxidative stress. TQ and small amounts of epoxy-TQ are generated from Toc in the liposome peroxidation model [23], during lipid peroxidation of isolated mitochondria [24] and in mitochondria of rat livers perfused with *tert*-butyl hydroperoxide [25]. TQ levels or the TQ/Toc ratios were found to be elevated in various tissues after exercise [20], hyperoxia [26], cigarette smoking [27] or aging [28], and in pathologies related to oxidative stress such as ethanol intoxication [18], ischemia/reperfusion injury [29], muscular dystrophy [30], diabetes [31] or atherosclerosis [32]. Therefore, TQ is increasingly used as a biomarker for oxidative stress. On the other hand, the function (if any) of this metabolite, particularly in mitochondria, is less clear. It has been considered as a mere waste product or as an essential cofactor for fatty acid desaturase in the mitochondrial outer membrane [33]. However, the most likely function favoured to date is that of an antioxidant in the reduced state, which is tocopheryl hydroquinone (tocopheryl quinol, TQH_2).

Since the submitochondrial distribution of TQ has not been reported yet and that of Toc shows tremendous literature variation (0–90% of the mitochondrial Toc have been found in

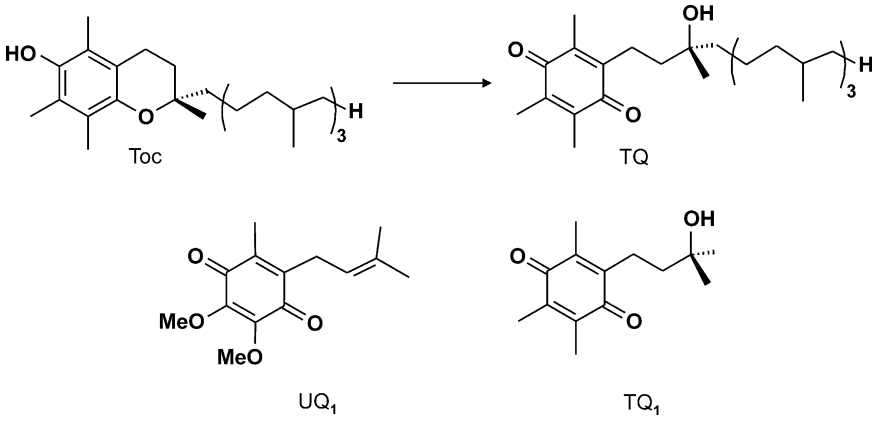

Scheme 1 – Structures of α-tocopherol (Toc), its oxidation product α-tocopheryl quinone (TQ) and the short-chain quinone homologues UQ_1 and TQ_1.

the outer membrane [16,34,35]), we decided to study the distribution of TQ over mitochondrial outer and inner membranes in comparison to Toc. In addition, information on the possible interference of TQ with ubiquinone-mediated redox processes is scarce. Particularly the question arises, how TQ could be reduced to TQH_2 in vivo. Therefore, we investigated the potential interference of TQ with ubiquinone functions at the mitochondrial complexes I, II and III. In addition, we studied the interaction of TQ with microsomal enzymes.

2. Materials and methods

2.1. Materials

UQ_1 and UQ_6 were obtained from Sigma. TQ and TQ_1 (2-(3-hydroxy-3-methyl-butyl)-3,5,6-trimethyl-[1,4]benzoquinone) were synthesized from all-rac α-tocopherol (Merck) and pentamethyl chromanol (Aldrich), respectively, as reported [17]. The short-chain quinols (UQ_1H_2 and TQ_1H_2) were prepared by reduction of the respective quinones with dithionite (dithionite/KBH_4 for TQ_1H_2) in ethanol/water (1:1) at pH 2 and subsequent extraction with anaerobic hexane.

2.2. Isolation of mitochondria

Rat heart mitochondria (RHM) were isolated from male Sprague–Dawley rats (Research Institute for Laboratory Breeding, Himberg, Austria) according to Ref. [36]. Rat liver mitochondria (RLM) were isolated using the same procedure with the following modifications: the preparation buffer (225 mM mannitol, 75 mM sucrose, 0.5 mM EGTA, 1 mM DETAPAC, 2 mM MOPS, pH 7.4 at 4 °C) was supplemented with 10 mg/l BHT to prevent tocopherol oxidation. One or two livers were homogenized in 60 ml buffer and the mitochondria were washed three times (in 120, 60 and 30 ml buffer, respectively). The protein concentration was measured with the Biuret method (BSA as standard).

2.3. Separation of mitochondrial membrane fractions

Mitoplasts (MP1) and mitochondrial outer membranes (OM1) were isolated with the digitonin method [37]: freshly prepared RLM1 (50 mg/ml protein in preparation buffer) were incubated with 0.2 mg digitonin per mg protein for 30 min under gentle stirring. After dilution with 3 volumes of buffer, MP1 were pelleted at 23,000 × *g* for 10 min and washed twice with buffer. Alternatively, MP2 and OM2 were isolated with the swelling/rupture method [38]: freshly prepared RLM2 were repelleted, washed with 30 ml 2 mM MOPS/0.5 mM EGTA, pH 7.4, and incubated in this buffer at 5 mg/ml protein for 20 min under gentle stirring, followed by 20 strokes in a Potter homogenizer with a tight pestle. MP2 were pelleted as above. For both methods, 3 ml of the last supernatant were loaded on a step gradient of 1 ml 1.9 M sucrose and 1 ml 1 M sucrose, both in MOPS/EGTA buffer. After centrifugation at 138,000 × *g* for 1 h in a SW 50.1 swing-out rotor, OM1 (digitonin method) and OM2 (swelling method) were collected from the 0–1 M interface, diluted with MOPS/EGTA buffer, pelleted at 146,000 × *g* for 1 h and resuspended in preparation buffer. RLM, MP and OM samples were stored in liquid nitrogen until analysis. All procedures were performed at 4 °C.

2.4. Preparation of submitochondrial particles (SMP) and microsomes

SMP were obtained from beef heart mitochondria by sonication as described in Ref. [39]. Microsomes were prepared from rat liver according to Ref. [40].

2.5. HPLC analysis

Two to five milligrams protein (RLM, MP, OM) in 1 ml H_2O were mixed with 5 mM SDS and 2 nmol UQ_6 (internal standard), and extracted with 3 ml anaerobic ethanol/hexane (2:5). Quinones and Toc were eluted from a Nova-Pak C18 column (Waters LC1 module) with 50 mM $NaClO_4$ in ethanol/methanol/acetonitrile/$HClO_4$ (400:300:300:1) at 1 ml min^{-1} and detected optically (268 nm for TQ, 275 nm for UQ) or electrochemically (+0.6 V, for Toc and UQH_2) [41]. For the quantification of FAD and FMN, 1 ml of the SMP suspension (10.5 mg protein) was extracted with 900 μl H_2O at 90 °C for 25 min. After centrifugation the extract was eluted from the C18 column with 20% methanol/80% 10 mM phosphate buffer (pH 5.2) at 1 ml min^{-1} (adopted from Ref. [42]). Flavins were analyzed with a Jasco FP-920 fluorescence detector (excitation 450 nm, emission 520 nm). The concentrations were calculated using external FAD and FMN standards.

2.6. UV–vis spectroscopy

UV spectra of 20 μM UQ_1 and UQ_1H_2 were measured under conditions of the kinetic measurements, i.e., in SMP-containing Tris buffer supplemented with KCN (vide infra) before and after complete reduction with 2 mM succinate, and an effective extinction coefficient $\varepsilon_{eff} = \varepsilon_{280-320}$ (UQ_1) − $\varepsilon_{280-320}$ (UQ_1H_2) of 11.4 ± 0.2 $mM^{-1}\,cm^{-1}$ was calculated from these spectra. Likewise, the spectrum of 12 μM TQ_1 (calculated from $\varepsilon_{268} = 19.5\ mM^{-1}\,cm^{-1}$ [20]) was measured in Tris buffer before and after reduction with about 1 mg KBH_4. An effective $\varepsilon_{eff} = \varepsilon_{280-288}$ (TQ_1) − $\varepsilon_{280-288}$ (TQ_1H_2) of 12.7 ± 0.3 $mM^{-1}\,cm^{-1}$ was calculated. Mitochondrial cytochromes *a* and *b* were quantified from dithionite-reduced minus air-oxidized difference spectra according to Ref. [43]. Difference spectra of cytochrome P-450 were measured as CO/reduced (bubbling with CO gas for 30 s) minus reduced (with a few grains of sodium dithionite) in 100 mM phosphate buffer (pH 7), using $\varepsilon_{450-490} = 91\ mM^{-1}\,cm^{-1}$ [44]. Cytochrome b_5 was quantified from the reduced (200 μM NADH) minus air-oxidized difference spectrum using $\varepsilon_{424-409} = 185\ mM^{-1}\,cm^{-1}$ [44].

2.7. Enzyme assays

Monoamine oxidase (MAO) and cytochrome oxidase (Cox) activities were measured at room temperature to assess MP and OM purity. The MAO assay contained 2 μM scopoletin, 0.1 mg/ml horseradish peroxidase (HRP), 1.5 mM benzylamine and 1 mM DETAPAC in 30 mM sodium phosphate buffer (pH 7.4). MAO-catalyzed H_2O_2 formation was measured fluorime-

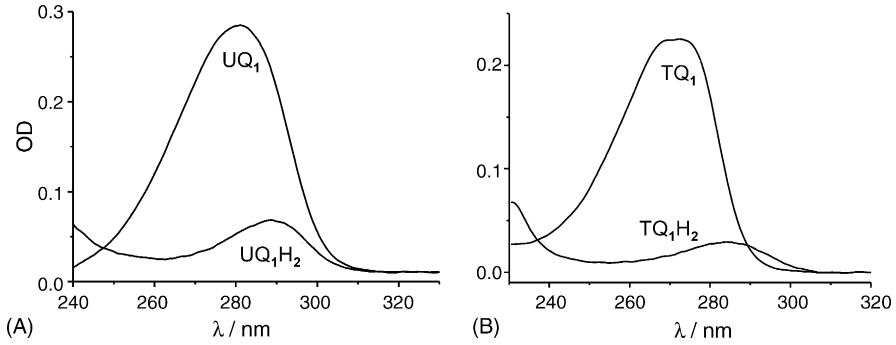

Fig. 1 – UV spectra of UQ_1/UQ_1H_2 (panel A) and TQ_1/TQ_1H_2 (panel B) in aqueous buffer (see Section 2).

trically as HRP-catalyzed scopoletin consumption. The fluorimeter (F-4500, Hitachi) was set to 366 nm excitation, 460 nm emission, 5/5 nm slit widths, 8 s response time and 700 V PMT voltage, and it was calibrated with 1 μM H_2O_2.

The following assays were measured on a DW 2000 spectrophotometer (Aminco) with the slit width set at 3 nm. The Cox assay contained 15 μM horse heart ferrocytochrome c in the same phosphate buffer. Cytochrome oxidation was followed at 550 − 540 nm. An $\varepsilon_{550-540}$ value of 19 mM^{-1} cm^{-1} was used [41].

Complex I (NADH:quinone oxidoreductase, NADH dehydrogenase, EC 1.6.5.3) activity was measured as the decay of NADH absorption at 340 − 410 nm at 25 °C in 20 mM Tris buffer (pH 7.5) [45] containing 170 μg/ml SMP, 100 μM NADH, 50 μM quinone (from a 10 mM ethanolic solution), 2 mM KCN and 20 μM antimycin A (0.2%, v/v acetonitrile). To measure the bulk phase Michaelis constant ($K_{M,app}$) and the maximal velocity (V_{max}), the reaction was started by addition of the indicated concentrations of UQ_1, UQ_6, TQ_1 or TQ (in ethanol) to an otherwise identical assay mixture that had been adjusted with ethanol to a final concentration of 1% (v/v). After about 40 s, the reaction was inhibited with 2 μg/ml rotenone (0.1%, v/v acetonitrile). Since this inhibition was less than 100%, especially at higher quinone concentrations [46], the residual activities were subtracted from the linear slopes prior to rotenone addition in order to assess the kinetic properties of the physiological quinone site. The corrected slopes were converted to reaction rates using an $\varepsilon_{340-420}$ value of 6.2 mM^{-1} cm^{-1} for NADH [47].

Complex II (succinate:quinone oxidoreductase, succinate dehydrogenase, EC 1.3.5.1) activity with UQ_1 as substrate was measured as the decay of UQ_1 absorption at 280 − 320 nm (using an ε_{eff} = 11.4 mM^{-1} cm^{-1}, vide supra) at 25 °C in 20 mM Tris buffer (pH 7.5) containing 170 μg/ml SMP, 2 mM succinate, 50 μM quinone (from a 10 mM ethanolic solution), 2 mM KCN and 20 μM antimycin A. SMP were preincubated with succinate and KCN for 6 min for maximal activation of the enzyme. Antimycin was added towards the end of this period, and the reaction was started by addition of quinone. Michaelis–Menten kinetics were measured in analogy to complex I, except complementing amounts of ethanol were added towards the end of the 6 min period, and rotenone was omitted. Complex II activities with TQ_1 were measured at 271 − 288 nm (isosbestic point, see Fig. 1) in the presence of 20 μM antimycin A (otherwise as for UQ_1).

UQ_1 and TQ_1 reduction by complex III (quinol:cytochrome c oxidoreductase, cytochrome c reductase, cytochrome bc_1 complex, EC 1.10.2.2) was measured as for complex II with the following modifications. Rates in the presence of antimycin were subtracted from those obtained in the absence of antimycin (but in the presence of 0.2%, v/v acetonitrile, the solvent for antimycin). TQ_1 reduction was measured at 280 − 288 nm (using an ε_{eff} = 12.7 mM^{-1} cm^{-1}, vide supra) to keep the absorption within the linear range. Non-linearity was not a problem for UQ_1 measurements, since the faster reaction decreased the quinone absorption into the linear range.

UQ_1H_2 and TQ_1H_2 oxidation by complex III was measured in 10 mM Tris buffer (pH 7.4) containing 50 mM KCl, 1 mM EDTA, 100 μg/ml SMP, 50 μM horse heart ferricytochrome c, 2 mM KCN [48] and various concentrations of the quinol (from an ethanolic solution; 1%, v/v final ethanol concentration). Cytochrome c reduction was followed at 550 − 540 nm ($\varepsilon_{550-540}$ = 19 mM^{-1} cm^{-1}) [41]. Only the fraction of the activity sensitive to 20 μM antimycin A, corrected for the inhibitory effect of the solvent (acetonitrile) alone, was used for analysis.

Kinetics of NADPH:cytochrome P-450 reductase (EC 1.6.2.4) and NADH:cytochrome b_5 reductase (EC 1.6.2.2) were measured as the decay of NAD(P)H absorption at 340 − 410 nm at 25 °C in 20 mM Tris buffer (pH 7.5) containing 71 μg/ml microsomes, 100 μM NAD(P)H and the indicated concentrations of UQ_1, UQ_6, TQ_1 or TQ. Ethanol was complemented as above.

3. Results

3.1. *Distribution of TQ, Toc and UQ over mitochondrial membranes*

Using freshly isolated liver mitochondria (RLM1, RLM2) from healthy rats, we separated the outer membrane (OM) from mitoplasts (MP; mitochondria lacking the OM and the soluble intermembrane fraction) with two established methods: the digitonin method yielding MP1 and OM1, and the swelling/rupture method yielding MP2 and OM2. We analyzed MP directly rather than inner membranes to avoid stressful conditions necessary for their preparation (such as sonication, which might result in partial Toc oxidation [49]). Table 1 shows the characterization of these fractions. The activities of marker enzymes (MAO for OM, Cox for MP) revealed that

Table 1 – Characterization of the purity of mitoplast (MP) and mitochondrial outer membrane (OM) fractions using the enzymatic activities of monoamine oxidase (MAO) and cytochrome oxidase (Cox)

Fraction	MAO (nmol H_2O_2 (min mg)$^{-1}$)	Cox (μmol Cyt c (min mg)$^{-1}$)
RLM1[a]	2.17 ± 0.21	0.51 ± 0.28
MP1[a]	0.05 ± 0.05	0.89 ± 0.60
OM1[a]	91 ± 11	1.61 ± 0.96
RLM2[b]	2.46 ± 0.75	0.46 ± 0.22
MP2[b]	0.32 ± 0.12	0.50 ± 0.15
OM2[b]	79 ± 44	0.05 ± 0.05

MP1 and OM1 were purified from RLM1 with the digitonin method; MP2 and OM2 were purified from RLM2 with the swelling/rupture method. Errors indicate S.D.
[a] $n = 4$.
[b] $n = 5$.

the purity of MP was higher with the digitonin method (MP1), while the purity of OM was higher with the swelling method (OM2). Specific (total protein-based) activities of MAO and Cox in OM and MP, respectively, approached those reported for fractionated RLM (MAO, 120 nmol H_2O_2 (mg min)$^{-1}$ after the first gradient [38]; Cox, about 2 μmol Cyt c (mg min)$^{-1}$ [50]). The reduced-minus-oxidized difference vis spectrum of OM2 (not shown) revealed the mitochondrial isoform of cytochrome b_5 with α, β and γ peaks at 557, 528 and 426 nm, respectively. From the spectrum (which is undistinguishable from the microsomal isoform [51]) this cytochrome was quantified to 0.16 ± 0.02 nmol (mg protein)$^{-1}$, based on $\varepsilon_{429-409} = 163\ mM^{-1}\ cm^{-1}$ [51]. This value is somewhat smaller than the one reported (0.39 nmol/mg) [51]. However, the microsomal marker cytochrome P-450 was undetectable in all fractions.

Table 2 lists the concentrations (on a protein basis) of Toc, TQ and the two UQ homologues UQ_9 and UQ_{10} in intact mitochondria (RLM) and mitochondrial membrane fractions (MP, OM) from rat liver, using HPLC analysis. Since the TQ/Toc ratio is frequently used as a biomarker for oxidative stress, it is included in the table, as is the analysis of intact mitochondria from rat heart (RHM) and rat liver microsomes for comparison. The microsome fractions had a cytochrome P-450 content of 1.24 ± 0.28 nmol (mg protein)$^{-1}$ and contained about 1% mitochondrial membranes, as estimated from its Cox activity.

3.2. Detection of substrates for kinetic measurements

For the assays used to determine the kinetic parameters of enzyme activities, the time-dependent detection of either the electron donor or the electron acceptor was required. In the case of NADH or NADPH as substrates, their decrease had to be measured since their strong UV absorption strongly overlaps with the quinone absorption bands. In contrast, in the case of succinate, which does not absorb in the region of quinone UV absorption, quinone reduction had to be measured directly. Since spectral parameters of quinones are mostly listed for ethanolic solutions in the literature [52], we compared the UV spectra of UQ_1 and UQ_1H_2 in conventional ethanolic solution (not shown) with those in aqueous buffer (Fig. 1). The peak of UQ is shifted from 275 nm in ethanol to 280 nm in the buffer. Since no isosbestic point is seen on the right side of the peak (cf. Ref. [53]), the baseline (320 nm) was chosen as reference. Likewise, the peak of TQ_1 is shifted from 268 nm in ethanol to 271 nm in the buffer. Contrary to UQ_1, a clear isosbestic point (288 nm) is seen.

3.3. Interaction of TQ with mitochondrial complex I

Complex I activities of submitochondrial particles (SMP) from beef heart were measured as the decay of NADH absorption at saturating concentrations (100 μM [46]). Fig. 2 shows slow, but concentration-dependent, rotenone-sensitive reduction of TQ. As a control, a ubiquinone homologue of comparable chain length (UQ_6 with six isoprenoid units, versus TQ with 4 units) was used. Within the linear range, the activity with UQ_6 was 14 times larger than that with TQ. For UQ_6 no saturation was found up to at least 300 μM bulk phase concentration. Likewise, the reduction of decyl-UQ showed no saturation up to 100 μM (not shown), although this frequently used UQ analogue is more hydrophilic than the natural UQ_9 or UQ_{10}. This demonstrates that reaction rates with hydrophobic long-chain quinones are generally limited by the rather slow transition between micelles and the membrane [46]. Therefore, the kinetics of TQ reduction were

Table 2 – HPLC analysis of rat liver and heart mitochondria (RLM and RHM), mitoplasts (MP) and outer membranes (OM) from RLM, and rat liver microsomes (micr.)

Fraction	Toc (nmol/mg)	TQ (nmol/mg)	TQ/Toc (mol%)	$UQ_{9,tot}$ (nmol/mg)	$UQ_{10,tot}$ (nmol/mg)
RLM1[a]	0.58 ± 0.20	0.0054 ± 0.0025	1.10 ± 0.69	1.28 ± 0.40	0.106 ± 0.040
MP1[a]	0.10 ± 0.02	0.0135 ± 0.0011	14.5 ± 2.8	1.23 ± 0.36	0.082 ± 0.025
OM1[a]	1.66 ± 0.32	0.0105 ± 0.0084	0.72 ± 0.72	2.06 ± 0.70	0.37 ± 0.14
RLM2[b]	0.68 ± 0.23	0.0104 ± 0.0053	1.71 ± 1.09	1.67 ± 0.93	0.16 ± 0.10
MP2[b]	0.19 ± 0.09	0.0022 ± 0.0008	1.56 ± 1.08	1.10 ± 0.35	0.10 ± 0.05
OM2[b]	1.51 ± 0.62	0.0100 ± 0.0089	0.75 ± 0.71	1.59 ± 1.03	0.27 ± 0.21
RHM[c]	1.68 ± 0.16	0.0325 ± 0.0035	1.94 ± 0.03	4.56 ± 0.61	0.29 ± 0.03
micr.[c]	0.59 ± 0.18	0.0170 ± 0.0080	2.73 ± 0.53	0.18 ± 0.09	0.025 ± 0.010

MP1 and OM1 were purified from RLM1 with the digitonin method; MP2 and OM2 were purified from RLM2 with the swelling/rupture method. Values are expressed in nmol (mg protein)$^{-1}$. Values for MP have been corrected for partial loss of soluble matrix proteins by comparing heme a concentrations per mg protein. UQ_{tot} values are the sum of the respective UQ and UQH_2 values. Errors indicate S.D.
[a] $n = 4$.
[b] $n = 5$.

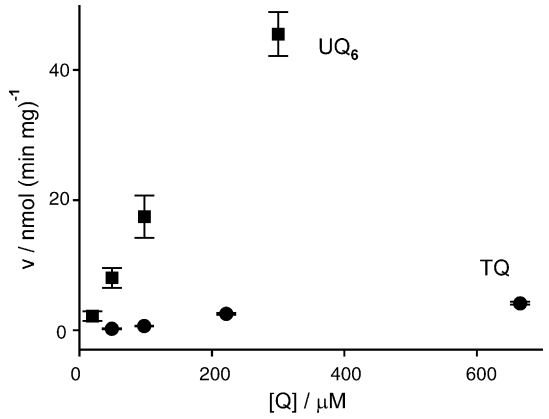

Fig. 2 – Saturation kinetics of mitochondrial complex I (NADH:quinone oxidoreductase) in beef heart submitochondrial particles with TQ (circles) and a medium-chain UQ homologue (UQ_6) (squares). Error bars indicate ±S.D.

studied in more detail using a more hydrophilic short-chain TQ homologue, TQ_1, and the corresponding UQ homologue, UQ_1 (Scheme 1). These kinetics (Fig. 3) were measured in the presence of antimycin A (a Q_i site inhibitor of complex III) to exclude interference from quinone reduction by complex III (vide infra) [46]. The lack of succinate-dependent TQ_1 reduction in the presence of antimycin A (vide infra) shows that electron transfer from endogenous UQH_2 to exogenous TQ_1 does not occur. Therefore, TQ_1 is directly reduced by complex I. Rotenone is known to bind competitively to the quinone pocket [5]. Therefore, the rotenone sensitivity of TQ_1 (50–70%) and UQ_1 (80–100%) reduction confirms binding to the physiological site. Residual, rotenone and antimycin A insensitive activity is not due to non-enzymatic reduction by NADH (not shown), but probably to an alternative reaction with complex I at a site upstream of the physiological site. This site was shown to interact also with other hydrophilic acceptors such as UQ_0 and ferricyanide [46], as well as with adriamycin [54]. Another likely contribution is NADH:cytochrome b_5 reductase activity distributed between the OM and microsomes [51]. TQ_1 was found to bind to the quinone pocket of complex I with five times lower affinity, compared to UQ_1 ($K_{M,app}$ 115 μM versus 23 μM, Table 3), and the maximal rate was 10 times smaller, comparing well with the 14 times larger activity with UQ_6 over TQ (vide supra). Partial inhibition of complex I at TQ_1 concentrations in excess of 400 μM (Fig. 3) might relate to the inhibitory effect of high UQ_2 concentrations [46].

3.4. *Interaction of TQ with mitochondrial complex II*

Measuring the decrease of quinone absorption (vide supra), we examined complex II activity in SMP. Fig. 4, panel A shows control experiments with UQ_1 in the presence of antimycin A as for complex I, yielding the kinetic parameters listed in Table 3. The partial decrease of activity seen at quinone concentrations in excess of 50 μM is reminiscent of the known complex I inhibition at high UQ_2 concentrations [46]. However, succinate-driven TQ_1 reduction was completely inhibited by antimycin A (Fig. 4, panel B) or stigmatellin (not shown), another complex III inhibitor. Thus, we could not detect direct TQ_1 reduction by complex II.

3.5. *Interaction of TQ/TQH_2 with mitochondrial complex III*

Similar to complex II, we studied quinone reduction by complex III. Fig. 5 shows the antimycin A sensitive UQ_1 and TQ_1 reduction. The latter is, in essence, a UQH_2:TQ transhydrogenase activity of complex III, where UQH_2 is the endogenous ubiquinol of the SMP preparation and TQ is the exogenous acceptor in excess over UQH_2. From the lack of succinate-dependent TQ_1 reduction in the presence of antimycin A we conclude, similar to above, that TQ_1 interacts directly with the quinone reduction site (Q_i pocket) of complex III. Reduction of short-chain UQ homologues and analogues by complex III has been observed before [46]. TQ_1 binds to complex III with comparable affinity, but with only 1% reactivity with respect to UQ_1 (Table 3).

We also investigated the reverse reaction, quinol oxidation by complex III with cytochrome c as electron acceptor. For TQ_1H_2 no antimycin-sensitive reaction was detectable under conditions employed for the UQ_1H_2 control (Fig. 6, Table 3).

3.6. *Interaction of TQ with cytochrome P-450 reductase*

In addition to cytochrome c, quinones are alternative substrates of the microsomal enzyme NADPH:cytochrome P-450 reductase [55]. Therefore, we also investigated NADPH-

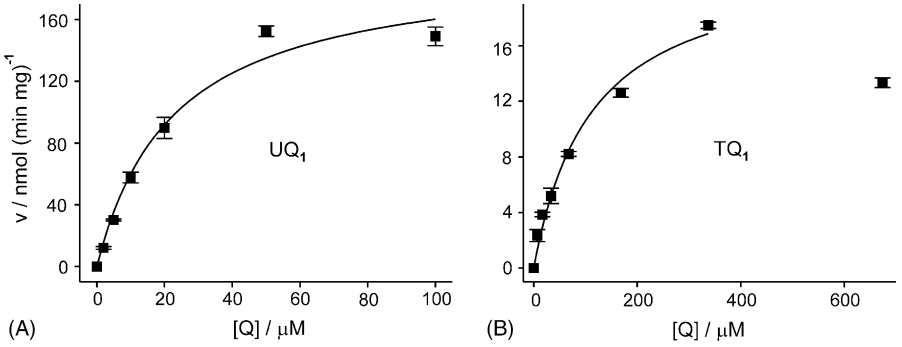

Fig. 3 – Saturation kinetics of mitochondrial complex I (NADH:quinone oxidoreductase) in beef heart submitochondrial particles with short-chain quinone homologues UQ_1 (panel A) and TQ_1 (panel B). The solid lines are fits according to the Michaelis–Menten equation (the data point at about 700 μM TQ_1 was excluded from the fit). Error bars indicate ±S.D.

Table 3 – Kinetic parameters for the reduction of short-chain quinone homologues UQ_1 and TQ_1 and for the oxidation of short-chain quinol homologues UQ_1H_2 and TQ_1H_2 by oxidoreductases in beef heart submitochondrial particles and rat liver microsomes

Enzyme	UQ_1				TQ_1			
	$K_{M,app}$ (μM)	V_{max} (nmol (mg min)$^{-1}$)	$k_{cat,app}$ (s^{-1})	$k_{cat,app}/K_{M,app}$ (s^{-1} μM^{-1})	$K_{M,app}$ (μM)	V_{max} (nmol (mg min)$^{-1}$)	$k_{cat,app}$ (s^{-1})	$k_{cat,app}/K_{M,app}$ (s^{-1} μM^{-1})
Complex I	22.8 ± 0.1[a]	260 ± 60[a]	39 ± 10	1.7	115 ± 3[a]	22.7 ± 0.1[a]	3.4 ± 0.1	0.03
Complex II	6 ± 1[a]	930 ± 210[a]	52 ± 12	8.6	n.r.	n.r.	n.r.	0
Complex III	22 ± 6[b]	610 ± 160[b]	19 ± 5	0.9	36 ± 2[a]	6.2 ± 0.6[a]	0.19 ± 0.02	0.005
P-450 red.	2.1 ± 0.1[a]	35 ± 1[a]	8.0 ± 0.3	3.8	12 ± 3[a]	39 ± 3[a]	8.9 ± 0.8	0.74
Cyt b_5 red.	97 ± 4[a]	105 ± 17[a]	53 ± 10	0.5	46 ± 12[a]	10 ± 2[a]	5.1 ± 1.2	0.11
	UQ_1H_2				TQ_1H_2			
Complex III	47 ± 6[a]	720 ± 100[a]	22 ± 3	0.5	n.r.	n.r.	n.r.	0

n.r.: no detectable reaction; P-450 red.: cytochrome P-450 reductase; Cyt b_5 red.: cytochrome b_5 reductase. Errors indicate S.D.
[a] $n = 2$.
[b] $n = 4$.

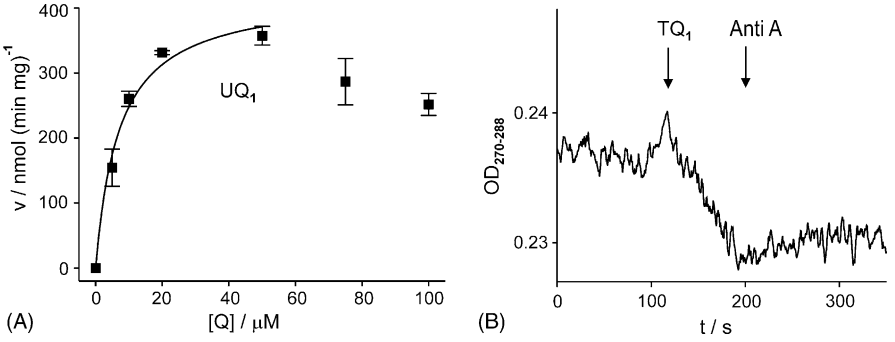

Fig. 4 – Panel A: saturation kinetics of mitochondrial complex II (antimycin A insensitive succinate:quinone oxidoreductase activity) in beef heart submitochondrial particles with the short-chain UQ homologue (UQ_1). The solid line is a fit according to the Michaelis–Menten equation (the data points at UQ_1 concentrations above 60 μM were excluded from the fit). Error bars indicate ±S.D. Panel B: succinate-driven reduction of the short-chain TQ homologue (TQ_1) and inhibition by antimycin A (Anti A).

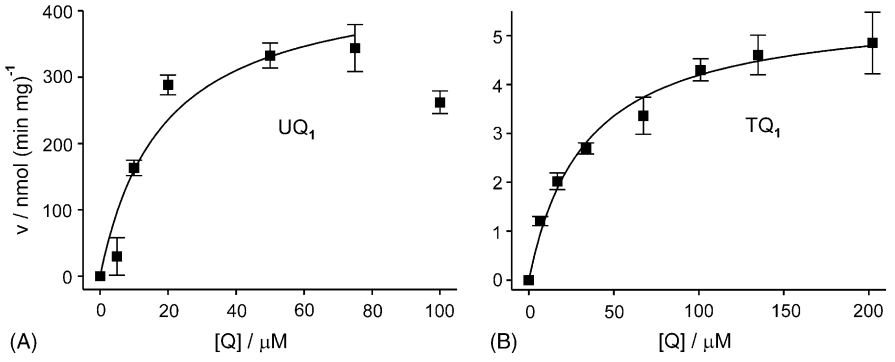

Fig. 5 – Saturation kinetics of mitochondrial complex III (antimycin A sensitive succinate:quinone oxidoreductase activity) in beef heart submitochondrial particles with short-chain quinone homologues UQ_1 (panel A) and TQ_1 (panel B). Succinate-driven quinone reduction at complex III was measured. The solid lines are fits according to the Michaelis–Menten equation (the data point at 100 μM UQ_1 was excluded from the fit). Error bars indicate ±S.D.

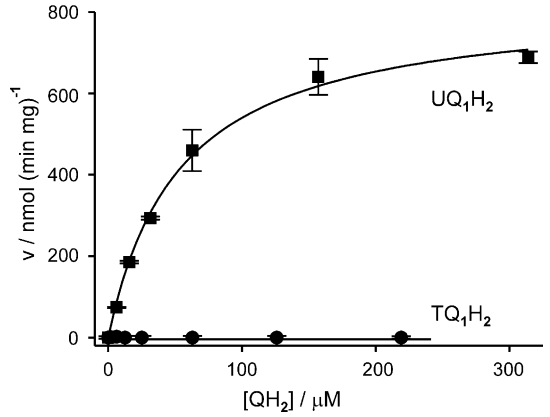

Fig. 6 – Saturation kinetics of mitochondrial complex III (quinol:cytochrome *c* oxidoreductase activity) in beef heart submitochondrial particles with short-chain hydroquinone (quinol) homologues (circles, TQ_1H_2; squares, UQ_1H_2). Quinol-driven cytochrome *c* reduction at complex III was measured. The solid lines are fits according to the Michaelis–Menten equation. Error bars indicate ±S.D.

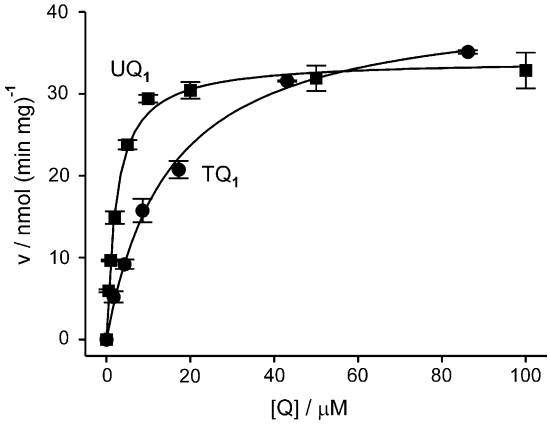

Fig. 7 – Saturation kinetics of microsomal cytochrome P-450 reductase (NADPH:quinone oxidoreductase) in rat liver microsomes with short-chain quinone homologues (circles, TQ_1; squares, UQ_1). The solid lines are fits according to the Michaelis–Menten equation. Error bars indicate ±S.D.

dependent TQ and UQ_6 reduction by rat liver microsomes. For TQ (150–450 μM) and UQ_6 (50–150 μM) we observed concentration-dependent reduction rates in the range of 4–5 and 2–3 nmol mg^{-1} min^{-1}, respectively (not shown). As for complex I, low solubilities of long-chain quinones precluded a detailed kinetic analysis. Fig. 7 shows that both TQ_1 and UQ_1 reacted with comparable rates, but TQ_1 affinity was 6 times lower (Table 3).

3.7. *Interaction of TQ with cytochrome b_5 reductase*

Quinones are also alternative substrates of the microsomal enzyme NADH:cytochrome b_5 reductase [55]. Both TQ_1 and UQ_1 showed NADH-dependent reduction by microsomes (Fig. 8). The activity was about 10 times lower with TQ_1, but with almost twice the affinity (Table 3).

In order to calculate turnover numbers ($k_{cat,app}$, Table 3) from maximal rates (V_{max}), the concentrations of the respective enzymes were obtained from HPLC and photometric measurements. From FMN, FAD and Cyt *b* analysis, concentrations of 0.110 ± 0.002 nmol/mg complex I, 0.303 ± 0.004 nmol/mg complex II and 0.535 ± 0.001 nmol/mg complex III, respectively, were obtained. Assuming a 1:15 ratio for Cyt P-450 reductase:-Cyt P-450 [56], a concentration of 0.073 nmol/mg Cyt P-450 reductase was calculated from 1.09 ± 0.02 nmol/mg Cyt P-450. Likewise, assuming a 1:10 ratio of Cyt b_5 reductase:Cyt b_5 [57], a concentration of 0.033 nmol/mg Cyt b_5 reductase was obtained from 0.33 ± 0.01 nmol/mg Cyt b_5.

4. Discussion

To test the origin and possible function(s) of TQ, we investigated its distribution over submitochondrial membrane fractions from livers of healthy rats and compared it to that of Toc and UQ. The total mitochondrial Toc concentrations we found (0.6–0.7 nmol/mg in RLM1 and RLM2, Table 2) are in the range reported before by us (1.2 nmol/mg [41]) and others (0.08–0.2 nmol/mg [58]; 0.24 nmol/mg [59]) for RLM, but larger than the 50 pmol/mg reported in Ref. [60]. Both separation methods yielded similar specific Toc contents in the MP and OM, respectively (Table 2). RLM have 68, 22, 6 and 4% of their total protein in the matrix, IM, intermembrane and OM fraction, respectively [50]. From this

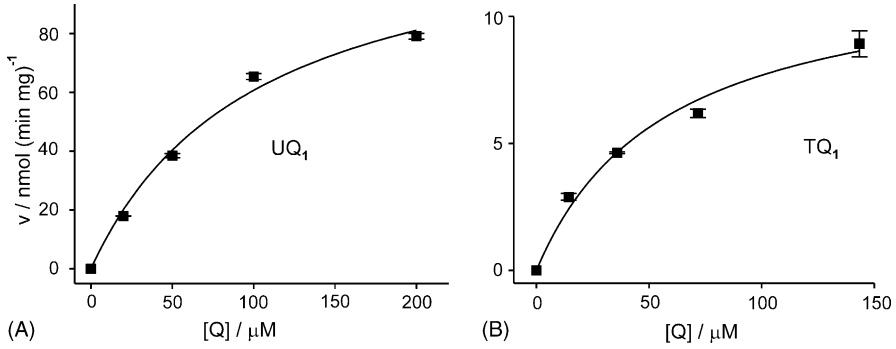

Fig. 8 – Saturation kinetics of microsomal cytochrome b_5 reductase (NADH:quinone oxidoreductase) in rat liver microsomes with short-chain quinone homologues UQ_1 (panel A) and TQ_1 (panel B). The solid lines are fits according to the Michaelis–Menten equation. Error bars indicate ±S.D.

one can calculate that the Toc contents of OM1 and OM2 constitute 42% and 26%, respectively, of the total mitochondrial membrane-bound Toc. Our results are similar to Ref. [61]. Zhang et al. [34] found about 10 times lower Toc levels, but also comparable specific concentrations in IM and OM, similar to Ref. [62] (1.3 times more Toc per lipid in OM than in IM). These data are in contrast to Ham and Liebler [16] who reported that about 90% of the mitochondrial Toc are localized in the OM. In the other extreme, Oliveira et al. [35] failed to detect any Toc in the OM from beef heart mitochondria.

The TQ concentrations we found in RLM (Table 2) are similar to those reported by us before (30 pmol/mg [41]) and others (4.5 pmol/mg [18]), but considerably smaller than the sum of TQ and TQH_2 (2 nmol/mg) reported in Ref. [63]. The specific TQ concentrations in MP and OM are very similar, except the decreased amount in MP2 (Table 2). To date, we have no explanation for this discrepancy. Since RLM have 68% and 22% of their total protein in the matrix and IM, respectively [50], MP values should be multiplied by 4 to obtain IM values for comparison with OM values on a membrane protein basis. Furthermore, the OM has a 1.8-fold smaller protein per lipid ratio than the IM [38]. This results in a nine-fold (digitonin method) and 1.6-fold (swelling method) higher TQ concentration in the IM on a lipid (or membrane area) basis. Larger steady state TQ concentrations in the IM are expected from the antioxidant function of Toc in respiratory electron transport, which occurs in this compartment. On the other hand, from this result the proposed function of TQ as an essential cofactor for fatty acid desaturase in the OM [33] cannot be excluded. The TQ/Toc ratio, often used as a marker for oxidative stress, varies from 0.7% to 15% (Table 2). Hayashi et al. reported ratios of 5–50% in whole liver homogenates [64], suggesting that higher ratios might be found in other cell fractions. However, the ratio we found in microsomes (Table 2) lies within the range found in mitochondria.

UQ_9 is the predominant UQ homologue in rodents. The values we found (Table 2) correlate well with the values previously reported by us [41] and others [34,58–60]. For RHM we found about three times higher concentrations of Toc and UQ, compared to RLM, similar to Ref. [59]. Accordingly, TQ levels were also higher. For liver microsomes, Toc values are comparable to RLM, whereas UQ levels are only about 10% (Table 2), in agreement with Ref. [34]. TQ values were also comparable to RLM.

Based on these data, TQ concentrations in mitochondria from healthy animals are about 1% of the UQ level. This ratio, however, is expected to increase under conditions of oxidative stress, examples of which have been given in the introduction. In addition, TQ-rich diet might have a similar effect, as shown by TQ accumulation in the isolated heart after perfusion with TQ [17], and in the liver after feeding TQ [65]. This prompted us to investigate the possible interference of TQ with (ubi)quinone-binding redox enzymes.

4.1. *Mitochondrial complex III*

We previously described interactions of the TQ/TQH_2 redox couple with mitochondrial complex III. TQH_2 was oxidized by SMP, but slower than $UQ_{10}H_2$ and without saturation [17]. For the oxidation of decyl-UQH_2 and TQ_1H_2 (termed TQ_0H_2 in this report) by complex III purified from beef heart we found V_{max} values of 290 and 0.5 s^{-1}, respectively, and $K_{M,app}$ values of 400 and 85 μM, respectively [41]. We reinvestigated this reaction using short-chain quinones and SMP. Obviously, the activity of TQ_1H_2 at the complex is so low that we have not been able to detect it in SMP (Fig. 6). The control parameters found for UQ_1H_2 ($K_{M,app}$ 47 μM, Table 3) were quite different from decyl-UQH_2 (although similar to the reported 13 μM [48]), probably due to differences between the isolated protein and native membranes.

In addition to quinol oxidation, complex III catalyzes quinone reduction in the course of the well-defined Q-cycle [66]. Complete antimycin A sensitivity of succinate-dependent TQ_1 reduction by SMP [17] was a first indication for TQ reduction by complex III. We previously showed that reduction of TQ_1 by prereduced b-cytochromes takes place at the Q_i (Q_{in}) site, whereas oxidation of TQ_1H_2 by oxidized b-cytochromes was more efficient at the Q_o (Q_{out}) site, in contrast to decyl-UQH_2 [41]. As a result of its binding to complex III with small reactivity, TQ acts as a weak competitive inhibitor, with 5% TQ_1 (with respect to decyl-UQH_2) inhibiting about 10% of the cytochrome reductase activity [41]. We now report kinetic details of the reduction of TQ_1 by complex III at the antimycin A sensitive Q_i site (Table 3). We found comparable affinities of both quinones, but TQ_1 reactivity was about 100 times smaller, again suggesting competitive inhibition by TQ_1.

We extended these studies to other quinone reductases. Generally, TQ reduction/TQH_2 oxidation effects are not due to electron exchange with endogenous UQ/UQH_2. Although the redox potential (E^0) of TQ (as adapted from its analogue duroquinone) is more negative than that of UQ (+50 mV versus +90 mV [41]), non-enzymatic quinol–quinone reactions (even between ubiquinol and ubiquinone) do not occur [67]. This we had specifically shown for TQH_2/UQ in an organic solvent at neutral pH [41] and by the lack of succinate-dependent TQ_1 reduction by SMP in the presence of antimycin A (Fig. 4, panel B). A likely explanation is that such reactions proceed at significant rates via deprotonated quinol/semiquinone anions, which must be stabilized by alkaline pH or, in biological systems, by specific protein interactions.

4.2. *Mitochondrial complex I*

We report rotenone-sensitive reduction of both TQ (Fig. 2) and short-chain TQ_1 (Table 3). The $K_{M,app}$ and V_{max} values for the UQ_1 control (Table 3) are similar to the literature values [46]. Hayashi et al. [64] also reported NADH-dependent TQ reduction by RLM, but without showing inhibitor specificities which would indicate enzyme(s) involved. Hughes and Tove [63] reported TQ reduction by RLM but detected neither antimycin A nor rotenone sensitivity, both (vide supra) in contradiction to our results. A similar quinone is duroquinone, which differs from TQ only by the lack of the side chain. This quinone was found to be largely reduced by complex III rather than complex I [46], but TQ_1 reduction by complex I was faster than its reduction by complex III (Table 3). Therefore, TQ_1 binding to quinone pockets of proteins seems to be modulated by the isoprenyl tail or, more likely, by the hydroxyl group at position 3′, a unique

feature of quinones which arise from oxidation of a chromanol such as Toc.

4.3. *Mitochondrial complex II*

The $K_{M,app}$ and V_{max} values for the UQ_1 control (Table 3) are virtually identical to the literature values [68]. The lack of activity of TQ_1 with this enzyme (Fig. 4, panel B) is in line with our previous report that succinate-dependent TQ_1 reduction by SMP was 100% sensitive to antimycin A (in contrast to UQ_1 and decyl-UQ [17]) and was thus catalyzed by complex III rather than complex II (vide supra). Succinate-dependent TQ reduction by RLM, reported by Hayashi et al. [64] (without investigating inhibitor effects) should be interpreted in view of this result.

4.4. *Microsomal cytochrome P-450 reductase*

In addition to its most important physiological function as NADPH:cytochrome P-450 reductase, this enzyme can reduce UQ to UQH_2 in a sequential two-electron transfer [69]. We found slow reduction of both TQ and UQ_6 (not shown). In addition we found comparable kinetics of this reaction with TQ_1 and UQ_1 (Table 3). In agreement with this are studies with the isolated enzyme: Hayashi et al. observed TQ reduction at a rate of about 10 μmol mg^{-1} min^{-1} [64]. Assuming a ratio of 130 between the specific activities of pure P-450 reductase and microsomes [70], this translates to a microsomal activity of 78 nmol mg^{-1} min^{-1}, a value similar to our V_{max} (Table 3). In line with the similar activities of complex I and P-450 reductase with TQ_1 (Table 3), other authors reported similar rates for a number of quinones [55], in agreement with the similar rates we found for TQ_1 and UQ_1 (Table 3).

4.5. *Microsomal cytochrome b_5 reductase*

NADH:cytochrome b_5 reductase is another microsomal enzyme capable of quinone reduction. We found that TQ_1 and UQ_1 bind with comparable affinity, but the reactivity of the former is only about 10%. This enzyme also catalyzed the reduction of the lipophilic TQ [71].

Taking together, our results show that the tolerance for binding of quinone structures different from the natural ubiquinone varies among quinone oxidoreductases. Comparing the maximal rates of the various reactions with UQ_1 and TQ_1 (Table 3), the selectivity of the quinone pockets, expressed as V_{max} (UQ_1)/V_{max} (TQ_1), decreases in the order: complex II > Q_o (complex III) > Q_i (complex III) > complex I ≈ Cyt b_5 reductase > P-450 reductase. Alternatively, the parameter k_{cat}/K_M is often used to characterize enzyme efficiency [46]. If $k_{cat,app}/K_{M,app}$ (Table 3) is used to calculate UQ_1/TQ_1 ratios, we obtain an almost identical order of selectivity. This correlates well with the order complex II > complex III > complex I, found with a number of UQ derivatives with different quinone ring substituents [47,72]. It is important to note that differences in reactivities do not necessarily match differences in binding which we estimated by measuring bulk phase $K_{M,app}$ values (Table 3). Although different from the true K_M values obtained from quinone concentrations in the membrane, these values reflect the relative binding affinities of quinones of similar hydrophobicity (similar chain length). Thus, TQ_1 and UQ_1 bind to the Q_i site of complex III with comparable affinity, yet the relative reactivity of TQ_1 is much smaller at complex III than at complex I (Table 3). This would make TQ a stronger competitive inhibitor at complex III than at complex I. At the same time, both enzymes contribute to the generation of some TQH_2.

Several other enzymes reacting with TQ/TQH_2 have been reported such as NAD(P)H:quinone oxidoreductase (DT-diaphorase) [73], cell membrane-bound enzymes from liver [74], xanthine oxidase [17] and carbonyl reductase [75]. In certain anaerobic bacteria a quinol (including TQH_2) dependent reduction of unsaturated fatty acids has been reported [76]. However, none of these proteins (including the ones investigated in the present study) is specific for TQ/TQH_2. They include either quinone-detoxifying enzymes with broad substrate range (DT-diaphorase) or UQ/UQH_2-dependent enzymes which show small activities with other quinones such as TQ, as discussed above.

Two effects emerge from these data: (i) the inhibition by TQ of enzymes interacting with quinones, for which both $K_{M,app}$ and V_{max} are small with respect to UQ and (ii) the generation of TQH_2. Several studies suggest that TQH_2 might function as an efficient antioxidant [73] or coantioxidant in combination with Toc [77], because it recycled Toc from its chromanoxyl radical faster than UQH_2 [78]. However, non-antioxidant functions of TQ (regulation of enzyme activity/gene expression), as have been described for Toc [79], cannot be ruled out. In any case, the homology of supernatant protein factor with α-TTP (Toc transfer protein), which is responsible for selective transport of α-Toc from the liver into other tissues [80], might indicate some need for TQ/TQH_2 in the body as well.

Acknowledgements

The technical assistance of Werner Stamberg is gratefully acknowledged. This work was supported by the Austrian Science Fund (FWF, Grant P16244-B08).

REFERENCES

[1] Batandier C, Fontaine E, Keriel C, Leverve XM. Determination of mitochondrial reactive oxygen species: methodological aspects. J Cell Mol Med 2002;6:175–87.
[2] Boveris A. Determination of the production of superoxide radicals and hydrogen peroxide in mitochondria. Methods Enzymol 1984;105:429–35.
[3] Gille L, Nohl H. The ubiquinol/bc_1 redox couple regulates mitochondrial oxygen radical formation. Arch Biochem Biophys 2001;388:34–8.
[4] Genova ML, Ventura B, Giuliano G, Bovina C, Formiggini G, Parenti-Castelli G, et al. The site of production of superoxide radical in mitochondrial complex I is not a bound ubisemiquinone but presumably iron-sulfur cluster N2. FEBS Lett 2001;505:364–8.
[5] Lambert AJ, Brand MD. Inhibitors of the quinone-binding site allow rapid superoxide production from mitochondrial NADH:ubiquinone oxidoreductase (complex I). J Biol Chem 2004;279:39414–20.

[6] Novgorodov SA, Gudz TI, Kushnareva YE, Roginsky VA, Kudrjashov YB. Mechanism accounting for the induction of nonspecific permeability of the inner mitochondrial membrane by hydroperoxides. Biochim Biophys Acta 1991;1058:242–8.
[7] Castilho RF, Kowaltowski AJ, Meinicke AR, Vercesi AE. Oxidative damage of mitochondria induced by Fe(II)citrate or t-butyl hydroperoxide in the presence of Ca^{2+}: effect of coenzyme Q redox state. Free Radic Biol Med 1995;18: 55–9.
[8] Brookes PS, Rolfe DF. The proton permeability of liposomes made from mitochondrial inner membrane phospholipids: comparison with isolated mitochondria. J Membr Biol 1997;155:167–74.
[9] Naumov VV, Khrapova NG. Chemiluminescent characteristics of ubiquinones. Biofizika 1985;30:5–9.
[10] Lass A, Sohal RS. Effect of coenzyme Q(10) and alpha-tocopherol content of mitochondria on the production of superoxide anion radicals. FASEB J 2000;14:87–94.
[11] Mukai K, Morimoto H, Kikuchi S, Nagaoka S. Kinetic study of free radical scavenging action of biological hydroquinones (reduced forms of ubiquinone, vitamin K and tocopherol quinone) in solution. Biochim Biophys Acta 1993;1157:313–7.
[12] Gregor W, Grabner G, Adelwohrer C, Rosenau T, Gille L. Antioxidant properties of natural and synthetic chromanol derivatives: study by fast kinetics and electron spin resonance spectroscopy. J Org Chem 2005;70:3472–83.
[13] Kagan V, Serbinova E, Packer L. Antioxidant effects of ubiquinones in microsomes and mitochondria are mediated by tocopherol recycling. Biochem Biophys Res Commun 1990;169:851–7.
[14] Moore AN, Ingold KU. α-Tocopheryl quinone is converted into vitamin E in man. Free Radic Biol Med 1997;22:931–4.
[15] Bello RI, Kagan VE, Tyurin V, Navarro F, Alcain FJ, Villalba JM. Regeneration of lipophilic antioxidants by NAD(P)H:quinone oxidoreductase 1. Protoplasma 2003;221:129–35.
[16] Ham AJ, Liebler DC. Vitamin E oxidation in rat liver mitochondria. Biochemistry 1995;34:5754–61.
[17] Gille L, Staniek K, Nohl H. Effects of tocopheryl quinone on the heart: model experiments with xanthine oxidase, heart mitochondria, and isolated perfused rat hearts. Free Radic Biol Med 2001;30:865–76.
[18] Kawase T, Kato S, Lieber CS. Lipid peroxidation and antioxidant defense systems in rat liver after chronic ethanol feeding. Hepatology 1989;10:815–21.
[19] Murphy ME, Kehrer JP. Simultaneous measurement of tocopherols and tocopheryl quinones in tissue fractions using high-performance liquid chromatography with redox-cycling electrochemical detection. J Chromatogr 1987;421:71–82.
[20] Mottier P, Gremaud E, Guy PA, Turesky RJ. Comparison of gas chromatography–mass spectrometry and liquid chromatography–tandem mass spectrometry methods to quantify alpha-tocopherol and alpha-tocopherolquinone levels in human plasma. Anal Biochem 2002;301:128–35.
[21] Hughes PE, Tove SB. Occurrence of alpha-tocopherolquinone and alpha-tocopherolquinol in microorganisms. J Bacteriol 1982;151:1397–402.
[22] Ibrahim WH, Bhagavan HN, Chopra RK, Chow CK. Dietary coenzyme Q_{10} and vitamin E alter the status of these compounds in rat tissues and mitochondria. J Nutr 2000;130:2343–8.
[23] Liebler DC, Burr JA. Antioxidant stoichiometry and the oxidative fate of vitamin E in peroxyl radical scavenging reactions. Lipids 1995;30:789–93.
[24] Vatassery GT, Smith WE, Quach HT. Increased susceptibility to oxidation of vitamin E in mitochondrial fractions compared with synaptosomal fractions from rat brains. Neurochem Int 1994;24:29–35.
[25] Ham AJ, Liebler DC. Antioxidant reactions of vitamin E in the perfused rat liver: product distribution and effect of dietary vitamin E supplementation. Arch Biochem Biophys 1997;339:157–64.
[26] Kanazawa H, Miyata C, Nagata Y, Urano S, Matsushima Y. Determination of alpha-tocopherol and alpha-tocopherylquinone in rat tissues and plasma by high-performance liquid chromatography with electrochemical detection. Chem Pharm Bull (Tokyo) 2000;48:1462–6.
[27] Wurzel H, Yeh CC, Gairola C, Chow CK. Oxidative damage and antioxidant status in the lungs and bronchoalveolar lavage fluid of rats exposed chronically to cigarette smoke. J Biochem Toxicol 1995;10:11–7.
[28] Yanagawa K, Takeda H, Egashira T, Sakai K, Takasaki M, Matsumiya T. Age-related changes in alpha-tocopherol dynamics with relation to lipid hydroperoxide content and fluidity of rat erythrocyte membrane. J Gerontol A 1999;54:B379–83.
[29] Murphy ME, Kolvenbach R, Aleksis M, Hansen R, Sies H. Antioxidant depletion in aortic crossclamping ischemia: increase of the plasma alpha-tocopheryl quinone/alpha-tocopherol ratio. Free Radic Biol Med 1992;13:95–100.
[30] Murphy ME, Kehrer JP. Altered contents of tocopherols in chickens with inherited muscular dystrophy. Biochem Med Metab Biol 1989;41:234–45.
[31] Shinozaki K, Takeda H, Inazu M, Matsumiya T, Takasaki M. Abnormal incorporation and utilization of alpha-tocopherol in erythrocyte membranes of streptozotocin-induced diabetic rats. Eur J Pharmacol 2002;456:133–9.
[32] Terentis AC, Thomas SR, Burr JA, Liebler DC, Stocker R. Alpha-tocopherol oxidation products in atherosclerotic leasions. Free Radic Biol Med 2001;31:S99.
[33] Infante JP. A function for the vitamin E metabolite alpha-tocopherol quinone as an essential enzyme cofactor for the mitochondrial fatty acid desaturases. FEBS Lett 1999;446:1–5.
[34] Zhang YY, Turunen M, Appelkvist EL. Restricted uptake of dietary coenzyme Q is in contrast to the unrestricted uptake of alpha-tocopherol into rat organs and cells. J Nutr 1996;126:2089–97.
[35] Oliveira MM, Weglicki WB, Nason A, Nair PP. Distribution of alpha-tocopherol in beef heart mitochondria. Biochim Biophys Acta 1969;180:98–113.
[36] Staniek K, Nohl H. H_2O_2 detection from intact mitochondria as a measure for one-electron reduction of dioxygen requires a non-invasive assay system. Biochim Biophys Acta 1999;1413:70–80.
[37] Rice JE, Lindsay JG. Subcellular fractionation of mitochondria. In: Graham JM, Rickwood D, editors. Subcellular fractionation, a practical approach. New York: Oxford University Press; 1997. p. 107–42.
[38] deKroon AIPM, Dolis D, Mayer A, Lill R, deKruijff B. Phospholipid composition of highly purified mitochondrial outer membranes of rat liver and Neurospora crassa. Is cardiolipin present in the mitochondrial outer membrane? Biochim Biophys Acta 1997;1325:108–16.
[39] Nohl H, Hegner D. Do mitochondria produce oxygen radicals in vivo? Eur J Biochem 1978;82:563–7.
[40] Murias M, Jäger W, Handler N, Erker T, Horvath Z, Szekeres T, et al. Antioxidant, prooxidant and cytotoxic activity of hydroxylated resveratrol analogues: structure–activity relationship. Biochem Pharmacol 2005;69:903–12.
[41] Gille L, Gregor W, Staniek K, Nohl H. Redox-interaction of alpha-tocopheryl quinone with isolated mitochondrial cytochrome bc_1 complex. Biochem Pharmacol 2004;68: 373–81.

[42] Arai K, Kanaseki T, Ohkuma S. Isolation of highly purified lysosomes from rat liver: identification of electron carrier components on lysosomal membranes. J Biochem 1991;110:541–7.
[43] Williams JN. A method for the simultaneous quantitative estimation of cytochromes a, b, c_1, and c in mitochondria. Arch Biochem Biophys 1964;107:537–43.
[44] Omura T, Sato R. The carbon monoxide-binding pigment of liver microsomes. I. Evidence for its hemoprotein nature. J Biol Chem 1964;239:2370–8.
[45] Bai Y, Attardi G. The mtDNA-encoded ND6 subunit of mitochondrial NADH dehydrogenase is essential for the assembly of the membrane arm and the respiratory function of the enzyme. EMBO J 1998;17:4848–58.
[46] Fato R, Estornell E, DiBernardo S, Pallotti F, Castelli GP, Lenaz G. Steady-state kinetics of the reduction of coenzyme Q analogs by complex I (NADH:ubiquinone oxidoreductase) in bovine heart mitochondria and submitochondrial particles. Biochemistry 1996;35: 2705–16.
[47] Ohshima M, Miyoshi H, Sakamoto K, Takegami K, Iwata J, Kuwabara K, et al. Characterization of the ubiquinone reduction site of mitochondrial complex I using bulky synthetic ubiquinones. Biochemistry 1998;37:6436–45.
[48] Fato R, Cavazzoni M, Castelluccio C, Castelli GP, Palmer G, Esposti MD, et al. Steady-state kinetics of ubiquinol cytochrome-c reductase in bovine heart submitochondrial particles—diffusional effects. Biochem J 1993;290: 225–36.
[49] Yumita N, Umemura S, Magario N, Umemura K, Nishigaki R. Membrane lipid peroxidation as a mechanism of sonodynamically induced erythrocyte lysis. Int J Radiat Biol 1996;69:397–404.
[50] Schnaitman C, Greenawalt JW. Enzymatic properties of inner and outer membranes of rat liver mitochondria. J Cell Biol 1968;38:158–75.
[51] D'Arrigo A, Manera E, Longhi R, Borgese N. The specific subcellular localization of two isoforms of cytochrome b_5 suggests novel targeting pathways. J Biol Chem 1993;268:2802–8.
[52] Hatefi Y. Coenzyme Q (Ubiquinone). Adv Enzymol 1963;25:275–328.
[53] Zweck A, Bechmann G, Weiss H. The pathway of the quinol quinone transhydrogenation reaction in ubiquinol—cytochrome-c reductase of neurospora mitochondria. Eur J Biochem 1989;183:199–203.
[54] Gille L, Nohl H. Analyses of the molecular mechanism of adriamycin-induced cardiotoxicity. Free Radic Biol Med 1997;23:775–82.
[55] Powis G, Appel PL. Relationship of the single-electron reduction potential of quinones to their reduction by flavoproteins. Biochem Pharmacol 1980;29: 2567–72.
[56] Shephard EA, Phillips IR, Bayney RM, Pike SF, Rabin BR. Quantification of NADPH: cytochrome P-450 reductase in liver microsomes by a specific radioimmunoassay technique. Biochem J 1983;211:333–40.
[57] Yang MX, Cederbaum AI. Interaction of ferric complexes with NADH-cytochrome b_5 reductase and cytochrome b_5: lipid peroxidation, H_2O_2 generation, and ferric reduction. Arch Biochem Biophys 1996;331:69–78.
[58] Lang J, Gohil K, Packer L. Simultaneous determination of tocopherols, ubiquinols and ubiquinones in blood, plasma, tissue homogenates and subcellular fractions. Anal Biochem 1986;1567:106–16.
[59] Kucharska J, Braunova Z, Ulicna O, Zlatos L, Gvozdjakova A. Deficit of coenzyme Q in heart and liver mitochondria of rats with streptozotocin-induced diabetes. Physiol Res 2000;49:411–8.
[60] Kamzalov S, Sohal RS. Effect of age and caloric restriction on coenzyme Q and alpha-tocopherol levels in the rat. Exp Gerontol 2004;39:1199–205.
[61] Thomas SM, Gebicki JM, Dean RT. Radical initiated α-tocopherol depletion and lipid peroxidation in mitochondrial membranes. Biochim Biophys Acta 1989;1002:189–97.
[62] Buttriss JL, Diplock AT. The relationship between alpha-tocopherol and phospholipid fatty-acids in rat-liver subcellular membrane-fractions. Biochim Biophys Acta 1988;962:81–90.
[63] Hughes PE, Tove SB. Synthesis of alpha-tocopherolquinone by the rat and its reduction by mitochondria. J Biol Chem 1980;255:7095–7.
[64] Hayashi T, Kanetoshi A, Nakamura M, Tamura M, Shirahama H. Reduction of alpha-tocopherolquinone to alpha-tocopherolhydroquinone in rat hepatocytes. Biochem Pharmacol 1992;44:489–93.
[65] Leray C, Wiesel ML, Freund M, Cazenave JP, Gachet C. Long-chain n-3 fatty acids specifically affect rat coagulation factors dependent on vitamin K: relation to peroxidative stress. Arterioscler Thromb Vasc Biol 2001;21:459–65.
[66] Crofts AR. The cytochrome bc_1 complex: function in the context of structure. Ann Rev Physiol 2004;66: 689–733.
[67] Cabrini L, Landi L, Pasquali P, Lenaz G. Effect of endogenous ubiquinone on the interaction of exogenous ubiquinone-1 with the respiratory-chain of bovine heart-mitochondria. Arch Biochem Biophys 1981;208:11–9.
[68] Fato R, DiBernardo S, Estornell E, Castelli GP, Lenaz G. Saturation kinetics of coenzyme Q in NADH oxidation: rate enhancement by incorporation of excess quinone. Mol Aspects Med 1997;18:S269–73.
[69] Sugioka K, Nakano M, Totsune-Nakano H, Minakami H, Tero-Kubota S, Ikegami Y. Mechanism of O_2^- generation in reduction and oxidation cycle of ubiquinones in a model of mitochondrial electron transport systems. Biochim Biophys Acta 1988;936:377–85.
[70] Yasukochi Y, Masters BSS. Some properties of a detergent-solubilized NADPH-cytochrome c (cytochrome-P-450) reductase purified by biospecific affinity chromatography. J Biol Chem 1976;251:5337–44.
[71] Nakamura M, Hayashi T. One- and two-electron reduction of quinones by rat liver subcellular fractions. J Biochem (Tokyo) 1994;115:1141–7.
[72] He DY, Gu LQ, Yu L, Yu CA. Protein–ubiquinone interaction: synthesis and biological properties of ethoxy ubiquinone derivatives. Biochemistry 1994;33:880–4.
[73] Siegel D, Bolton EM, Burr JA, Liebler DC, Ross D. The reduction of alpha-tocopherylquinone by human NAD(P)H: quinone oxidoreductase: the role of alpha-tocopherylhydroquinone as a cellular antioxidant. Mol Pharmacol 1997;52:300–5.
[74] Sun IL, Sun EE, Crane FL, Morre DJ, Lindgren A, Löw H. Requirement for coenzyme Q in plasma membrane electron transport. Proc Natl Acad Sci USA 1992;89: 11126–30.
[75] Wermuth B. Purification and properties of an NADPH-dependent carbonyl reductase from human brain. Relationship to prostaglandin 9-ketoreductase and xenobiotic ketone reductase. J Biol Chem 1981;256: 1206–13.
[76] Hughes PE, Tove SB. Identification of an endogenous electron donor for biohydrogenation as alpha-tocopherolquinol. J Biol Chem 1980;255:4447–52.
[77] Shi H, Noguchi N, Niki E. Comparative study on dynamics of antioxidative action of alpha-tocopheryl hydroquinone, ubiquinol, and alpha-tocopherol against lipid peroxidation. Free Radic Biol Med 1999;27:334–46.

[78] Mukai K, Itoh S, Morimoto H. Stopped-flow kinetic study of vitamin E regeneration reaction with biological hydroquinones (reduced forms of ubiquinone, vitamin K, and tocopherolquinone) in solution. J Biol Chem 1992;267:22277–81.
[79] Zingg JM, Azzi A. Non-antioxidant activities of vitamin E. Curr Med Chem 2004;11:1113–33.
[80] Blatt DH, Leonard SW, Traber MG. Vitamin E kinetics and the function of tocopherol regulatory proteins. Nutrition 2001;17:799–805.